International Journal of Engineering Research
Volume No.4, Issue No.4, pp : 173-177
ISSN:2319-6890)(online),2347-5013(print)
01 April 2015

Effect of Pipe Configurations on Air Entrainment into a Louvered Cylindrical Pipe: A Comparison between Open and Close Entrance of a Pipe

S.R. Sahu, D. P. Mishra*
Department of Mechanical Engineering, Birla Institute of Technology Mesra, Ranchi, 835215, India
kaisam.sameer@gmail.com,* dpmishra@bitmesra.ac.in

Abstract :The present numerical study was performed by solving conservation equations of mass, momentum and energy along with two equation based k-ε model for a louvered horizontal cylindrical pipe by finite volume method. It was found that pipe air suction increased with increase in opening area and number of nozzles for both pipe configurations. Increasing the pipe diameter made air suction more effective in pipe configuration B (open entrance of the pipe).

Keywords: entrainment, louvers, nozzle, exhaust gas, horizontal pipe

I. Introduction

Release of hot exhaust gases (temperature of about 70 ^{o}C) directly into the atmosphere is causing various environmental problems like smog formation and constant increase in atmospheric temperature. If the exhaust gases can be cooled, then the environment can be protected from its adverse effects. The cooling of exhaust gases can be done by sucking fresh air from the atmosphere through louvers of the pipe. Some research work was conducted in the past both theoretically and experimentally to overcome the harmful effects of release of hot exhaust gas. Han and Mungal (2001) in their study found that the increase in co-flow speed reduces the entrainment for both reacting and non-reacting jets. They also found that the entrainment in the near field of reacting jets was reduced by a factor of 2.5 due to the heat release effect. Mishra and Dash (2010) in their numerical investigation found that air suction rate is enhanced with increase in louvers opening area but independent of number of louvers per row. Singh et. al. (2010) found in their research that the ratio of tube diameter and inlet jet diameter along with the ratio of free stream air density to density of air at jet inlet condition were the main factors that influenced the entrainment and mixing. Barik et al. (2014) in an experimental and numerical investigation on air entrainment in infra-red suppression device found that the entrainment rate was reduced by 19.2% as the ratio of funnel overlap height and nozzle diameter changed from 0 to 1.6. Singh et al. (2003) in an experimental investigation found that non circular jets provided greater entrainment and mixing with ambient fluid than circular jets. They concluded that by shifting the location of jet, the entrainment was enhanced by 30%.

The work found in the literature does not site the use of CFD methods to determine the effect of various parameters on mass suction rate of air into a horizontal louvered pipe for a vehicle, and hence the present work is done to arrive at the optimum design of the pipe by investigating fluid flow and heat transfer characteristics. The study is carried out assuming exhaust pipe as the nozzle and hot air as the nozzle fluid and treated to be incompressible. We have attempted to match the existing experiment results of Singh et. al. (2003) with the present computational methods.

II. Mathematical Formulation

A cylindrical pipe of diameter D_P and length L_P was used to carry out the computational investigation. The pipe is closed at the entrance end and its exit end is open to the surrounding atmosphere for Configuration A whereas for Configuration B, both the ends of the pipe are open to the atmosphere. A nozzle of diameter D_n having a protrusion length L_{Pt} (into the pipe), is located at the centre of the entrance face of the pipe. A cylindrical computational domain of diameter D_{CD} (about 6 times of D_P) and length L_{CD} (about 3 times of L_P) is placed around the pipe so that the boundary conditions can be applied on the computational domain for the air to be sucked in by the louvers in the pipe. The louvers are made in circular shape (D_h = 0.03 m). A total of 12 louvers are placed in each stack with a distance of 0.5 m being maintained between each stack. The flow field in the domain is computed by using three-dimensional, incompressible Navier-Stokes equations and a standard two equation k-ε turbulence model with energy equation. The two equation k-ε turbulence model is believed to give the correct results for such Re flows. The fluid used for simulation is air at 343 K with a mass flow rate of 0.02 kg/s at nozzle outlet for every case and is treated as incompressible. Steel is declared as the solid material used for all the walls used for the present numerical research.

Governing Equations

The governing equations used for the present analysis can be written as:

Continuity equation:

$$\frac{\partial}{\partial x_i}(\rho U_i) = 0 \tag{1}$$

Momentum equation:

$$\frac{D(\rho U_i)}{Dt} = -\frac{\partial p}{\partial x_i} + \frac{\partial}{\partial x_j}[\mu(\frac{\partial U_i}{\partial x_j} + \frac{\partial U_j}{\partial x_i}) - \overline{\rho u_i u_j}] \tag{2}$$

$$\frac{p}{\rho} = RT \tag{3}$$

The density ρ is taken as the function of temperature according to the ideal gas law as per equation (3), while dynamic viscosity μ and thermal conductivity are kept constant.

Energy equation:

$$\frac{D(\rho T)}{Dt} = \frac{\partial}{\partial x_i}[(\frac{\mu}{\Pr} + \frac{\mu_t}{Pr_t})\frac{\partial T}{\partial x_i}] \tag{4}$$

ISSN:2319-6890)(online),2347-5013(print)
01 April 2015

Turbulence kinetic energy, k:

$$\frac{D}{Dt}(\rho k) = D_k + \rho P - \rho\varepsilon \quad (5)$$

Dissipation rate of k:

$$\frac{D}{Dt}(\rho\varepsilon) = D_\varepsilon + C_{1\varepsilon}\rho P\frac{\varepsilon}{k} - C_{2\varepsilon}\rho\frac{\varepsilon^2}{k} \quad (6)$$

$$\overline{u_i u_j} = \frac{2}{3}k\delta_{ij} - \nu_t\left(\frac{\partial U_i}{\partial x_i} + \frac{\partial U_j}{\partial x_i}\right) : \nu_t = 0.09\frac{k^2}{\varepsilon} \quad (7)$$

$$D_\phi = \frac{\partial}{\partial x_j}\left[\left(\mu + \frac{\mu_t}{\sigma_\phi}\right)\frac{\partial\phi}{\partial x_j}\right] \quad (8)$$

$$P = -\overline{u_i u_j}\frac{\partial U_i}{\partial x_j} \quad (9)$$

σ_k and σ_ε are the Prandtl numbers for k and ε.
R is characteristic gas constant and is equal to 0.287 kJ/kg-K.
The following constants are used in the k-ε equations.
$C_{1\varepsilon} = 1.44$, $C_{2\varepsilon} = 1.92$, $C_\mu = 0.09$, $\sigma_k = 1.0$, $\sigma_\varepsilon = 1.3$, $Pr_t = 1$.
Although these constants are normally used for internal flows, Fluent's default constants have not been changed for the present case of mixed flows, i.e. both internal and external.

Boundary Conditions

The boundary conditions for the louvered pipe can be seen from Fig. 1. The pipe and nozzle walls are solid and a no-slip boundary condition has been imposed. Pressure outlet boundary condition has been given to the top, side and bottom surface of the computational domain. Nozzle outlet has been given velocity inlet and temperature boundary condition to supply hot air into the pipe. The velocity will be computed from the local pressure field to satisfy continuity at the pressure outlet boundary while all the other variables like T, k and ε will be computed from zero gradient condition.
The turbulent intensity at nozzle inlet has been set to 2%, while 5% has been set for back flow turbulent intensity at all pressure outlet boundaries.

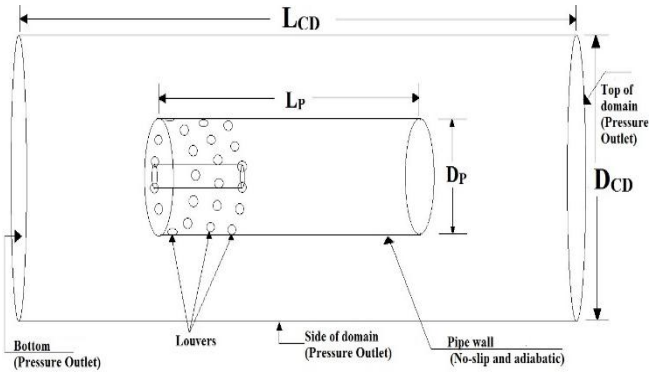

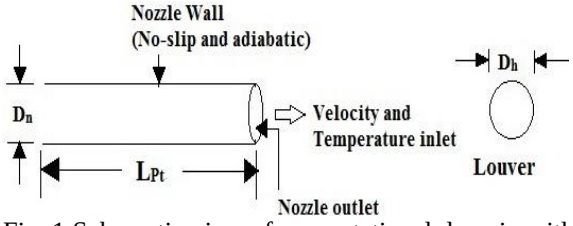

Fig. 1 Schematic view of computational domain with applied boundary conditions

III. Numerical Solution Procedure

The computational domain was discretized by using tetrahedral cells. The three dimensional equations for mass, momentum and energy were discretized over control volume using finite volume technique to obtain a set of algebraic equations. These algebraic equations were solved by algebraic multi grid solver of Fluent 14 by iteration using the imposed boundary conditions stated earlier. First order upwind scheme was considered for discretized momentum and turbulent equations. The effect of domain size and number of grids has been discussed in detail separately in the results and discussions.
The SIMPLE algorithm with Standard scheme was used for the pressure velocity coupling. Under relaxation factors of 0.3 for pressure, 0.7 for momentum, 0.8 for k and ε and 1 for temperature were used for the convergence of all variables. Fine grids were used at the nozzle entrance and louver openings to get better accuracy. Tetrahedral cells were used for the entire computational domain. Convergence criterion for the discretized equations for the whole field residual was set to 10^{-3} for all variables except for energy equation, whose residual level was set to 10^{-6}.

IV. Results and Discussions

Comparison with other computations

The ratio $Q_{suction}/Q_{inlet}$ obtained from numerical computation using k-ε turbulence model was compared with the experiment from Singh et. al. (2003) and Pritchard's relation for confined jet as can be seen from Fig. 2. The results from the present CFD k-ε model match well with the analytic solution developed by Pritchard (1977) and experiment from Singh et. al. (2003). The radial profile of mean axial velocity of a wall-constraint jet can be seen from Fig. 3. The mean axial velocity u(x, y) is normalised by the centreline velocity u(x, 0) and the radial distance is scaled by the jet half width ($y_{0.5}$). The jet half-width is defined as the transverse distance from the jet axis to the location where the mean axial velocity u(x, y) is half of the centreline value u(x, 0). Singh et. al. (2003) and Becker et. al. (1963) proposed that if the velocity profile exhibits self-similarity, then the axial velocity profile will be reduced into a single curve. From Fig. 3, it can be seen that the results from the present CFD k-ε model for radial profiles matches well with the experimental results from Singh et. al. (2003) and the empirical relation developed by Becker et. al. (1963). It was also possible to match the variation of entrainment ratio $Q_{suction}/Q_{inlet}$ as a function of jet location for a circular jet from the experimental results available from Singh et. al. (2003) with the present CFD k-ε model as can be seen from Fig. 4.

ISSN:2319-6890)(online),2347-5013(print)
01 April 2015

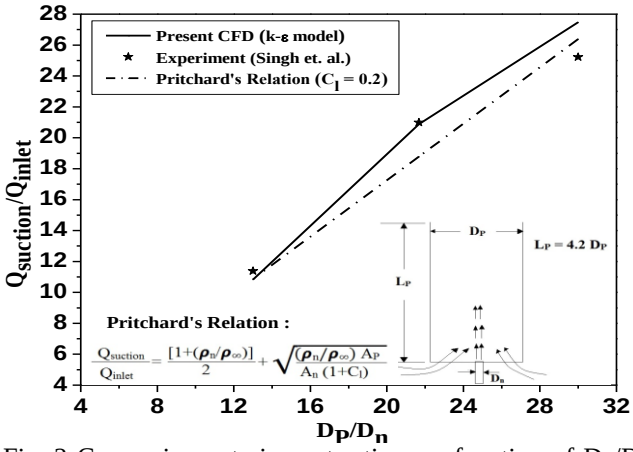

Fig. 2 Comparing entrainment ratio as a function of D_P/D_n for present CFD model with Pritchard's relation and experiment by Singh et. al.

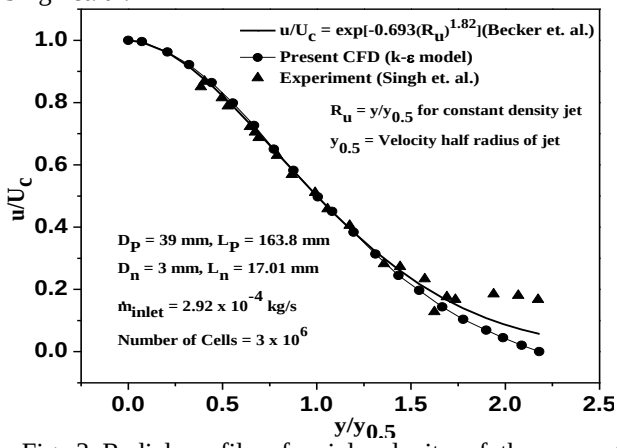

Fig. 3 Radial profile of axial velocity of the present CFD model compared with empirical correlation developed by Becker et. al.

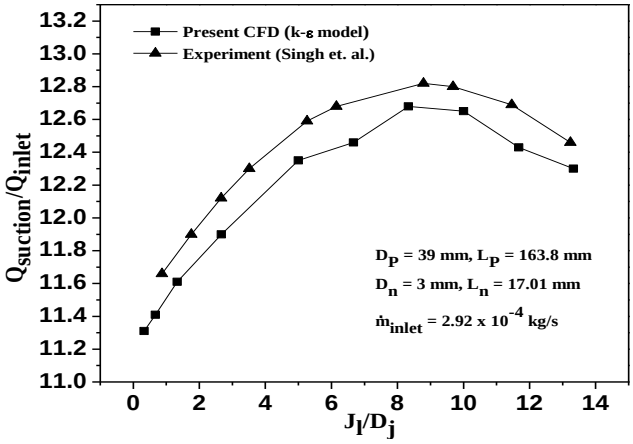

Fig. 4 Variation of entrainment ratio with jet location

Effect of louvers opening area on air suction rate

Fig. 7 and Fig. 8 show the effect of increasing opening area on air suction rate as a function of nozzle fluid temperature for pipe Configuration A and B. The area of each row of louver was kept constant at 0.0085 m^2 and keeping the area of the entrance face of the pipe constant at 0.03142 m^2. For pipe Configuration A only louver opening area was considered while for pipe Configuration B area of the entrance face was considered in addition to louver opening area. The simulations were carried out by increasing the rows of louvers up to 10 symmetrically around the periphery maintaining a distance of 0.05 m between each row. All the other parameters were kept constant as can be seen in the figure. From Fig. 7 and 8, it is clearly seen that by increasing the opening area, the air suction rate increased with a decrease in pipe outlet temperature. But after a certain opening area (about 0.051 m^2 for Configuration A and about 0.09 m^2 for Configuration B) there was no appreciable change in air suction rate because of the fact that the louvers located towards the top of the pipe do not create enough low pressure inside the pipe for the atmospheric air to be sucked in.

As atmospheric pressure was imposed on the top surface of the pipe, the louvers placed close to the top were not very effective compared to the louvers placed at the entrance half of the pipe. The streams of hot air from the nozzle (temperature about 70-80 ^{o}C) and the atmospheric air (temperature about 27 ^{o}C) got mixed inside the pipe and left from the top surface of the pipe.

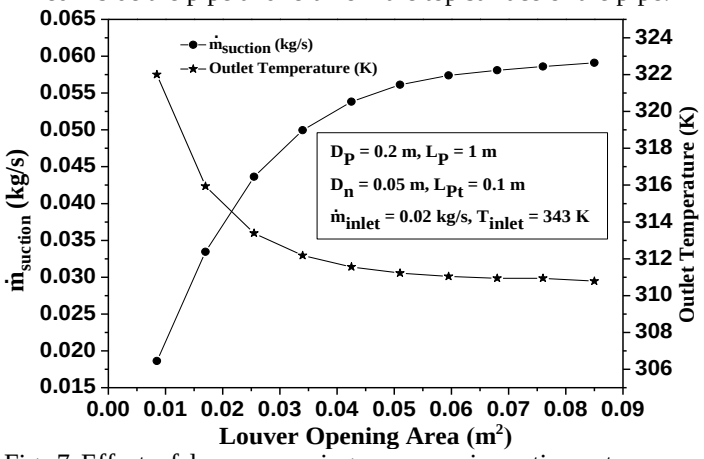

Fig. 7 Effect of louver opening area on air suction rate as a function of pipe outlet temperature

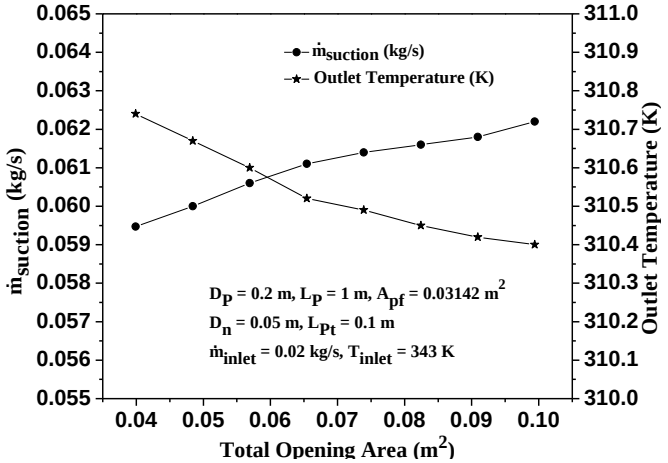

Fig. 8 Effect of total opening area on air suction rate as a function of pipe outlet temperature

Effect of number of nozzles on air suction rate

Fig. 9 shows the effect of number of nozzles on air suction rate as the function of nozzle fluid temperature. The simulation was

ISSN:2319-6890)(online),2347-5013(print)
01 April 2015

carried out for 1, 2, 4 and 6 nozzles. When single nozzle was used, it was located at the centre of the entrance face of the pipe. A constant pitch circle diameter (D_{pd} = 0.1 m) was used for placing the nozzles when the number of nozzles was increased to 2, 4 and 6. For single nozzle, the nozzle diameter was taken as 0.05 m. In order to maintain a constant mass flow rate and total cross section area of the nozzle, the diameters for 2, 4 and 6 nozzles were taken as 0.035 m, 0.025 m and 0.02 m. The simulation was carried out by keeping other parameters constant which can be seen in the figure. It was seen that when the nozzle number is increased to 6, the entrainment rate was increased to 1.1 times and there is sharp decrease in outlet temperature. As the number of nozzles increased the low pressure is created uniformly inside the pipe and suction rate is becoming more. Also there is chance of better mixing of the hot and cold fluid inside the pipe, so the outlet temperature of pipe falls for both the pipe configurations when the number of nozzle increased to 6.

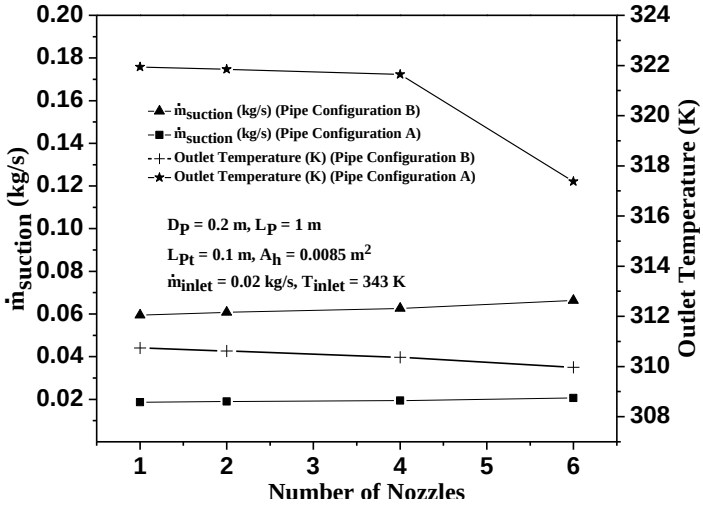

Fig. 9 Effect of number of nozzles on air suction rate as a function of pipe outlet temperature

Effect of change in pipe diameter on air suction rate

Figure 10 shows the effect of change in pipe diameter normalised by nozzle diameter on air suction rate as a function of nozzle fluid temperature. The louver opening area, pipe length, nozzle diameter and protrusion length mass flow rate and inlet temperature of nozzle fluid were kept constant as can be seen from the figure. The pipe diameter is increased from 0.15 m to 0.2 m. It is seen from the figure that with the increase in pipe diameter, there is a decrease in air suction rate for configuration A due to which the outlet temperature of the nozzle fluid increases whereas the case is opposite for configuration B. For pipe configuration B, the entrance face of the pipe is open to atmosphere, which increases the opening area allowing more air to be sucked into the pipe and reducing the pipe outlet temperature.

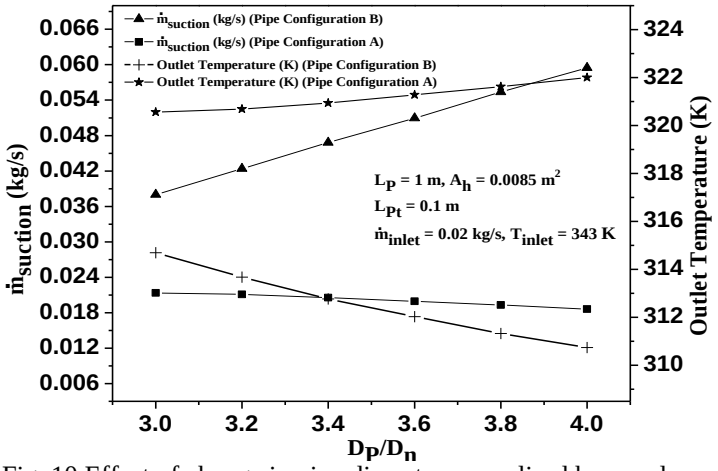

Fig. 10 Effect of change in pipe diameter normalised by nozzle diameter on air suction rate as a function of pipe outlet temperature

Conclusion

The conclusions that can be drawn from the present investigation are as follows:

- The air suction rate increased with the increase in louver opening area which thereby decreased the outlet temperature of the nozzle fluid. From the CFD analysis, it became clear that maximum suction effect was observed when the louvers were placed at the entry half of the pipe and closer to the nozzle. The air suction rate strongly depends on the opening area for both pipe configurations but minimum temperature was obtained in configuration B.
- The air suction rate is increased up to 1.1 times by using 6 nozzles as compare to single nozzle for both pipe configurations.
- For a given nozzle flow rate and opening area, it was found that the air suction rate decreased for configuration A whereas increased for configuration B when the pipe diameter was increased.

Nomenclature

A_h = Louvers opening area
A_{pf} = Area of entrance face of pipe
$C_{1\varepsilon}$ = Constant of value 1.44
$C_{2\varepsilon}$ = Constant of value 1.92
D_{CD} = Diameter of computational domain
D_p = Diameter of pipe
D_n = Diameter of nozzle
D_j = Diameter of jet
D_h = Diameter of circular louver
D_{pd} = Pitch circle diameter
$D_k = \frac{\partial}{\partial x_j}[(\mu + \frac{\mu_t}{\sigma_k})\frac{\partial k}{\partial x_j}]$
$D_\varepsilon = \frac{\partial}{\partial x_j}[(\mu + \frac{\mu_t}{\sigma_\varepsilon})\frac{\partial \varepsilon}{\partial x_j}]$
L_{CD} = Length of computational domain
L_p = Length of pipe
L_{Pt} = Protruding length of nozzle
J_l = Jet Location
$\dot{m}_{inlet}$ = Mass flow rate through the nozzle
$\dot{m}_{suction}$ = Air suction rate through louvers

ISSN:2319-6890)(online),2347-5013(print)
01 April 2015

k = Turbulent kinetic energy
P = Pressure
Pr = υ/α
Pr_t = Turbulent Prandtl number
Re_n = Reynolds number based on nozzle, $\rho V_n D_n/\mu$
T = Temperature
U = Velocity
V_n = Velocity at nozzle exit

Greek Symbols

υ = Kinematic Viscosity
ρ = Density
μ = Shear viscosity
μ_t = Turbulent viscosity
ε = Dissipation rate
σ_k = Turbulent Prandtl number for k
σ_ε = Turbulent Prandtl number for ε
ϕ = Scalar variable either k or ε
α = Thermal diffusivity

Subscripts

n = Nozzle
∞ = Free stream

References

i. F.P. Ricou and D.B. Spalding, "Measurements of entrainment by axisymmetrical turbulent jets," Journal of Fluid Mechanics 11, 21–32 (1981).

ii. B.J. Hill, "Measurement of local entrainment rate in the initial region of axisymmetric turbulent air jets," Journal of Fluid Mechanics 51, 773-779 (1972).

iii. D. Han and M.G. Mungal, "Direct measurement of entrainment in reacting/nonreacting turbulent jets," Combustion Flame 124, 370-386(2001).

iv. D.P. Mishra and S.K. Dash, "Numerical investigation of air suction through louvers of a funnel due to high velocity air jet," Computers & Fluids 39, 1597–1608(2010).

v. D.P. Mishra, S. K. Dash and P.A. Kishan, "Isothermal jet suction through the lateral openings of cylindrical funnel," Journal of Ship Research 54, 268-280(2010).

vi. G.S. Singh, T. Sundarajan and U.S.P. Shet, "Entrainment and mixing studies for a variable density confined jet," Numerical Heat Transfer, Part A. 35, 205-223 (2010).

vii. A. K. Barik, S. K. Dash and A. Guha, "Experimental and numerical investigation of air entrainment into an infrared suppression device," In press (2014)

viii. A. K. Barik, S. K. Dash, P. Patro and S. Mohapatra, "Experimental and numerical investigation of air suction into a louvered funnel," Appplied Ocean Research 48, 176-185 (2014).

ix. D. P.Mishra and S. K. Dash, "Maximum air suction into a louvered funnel through optimum design," Journal of Ship Research. 55, 1-11 (2011).

x. G. S. Singh, T. Sundarajan and K.A. Bhaskaran, "Mixing and entrainment characteristics of circular and non-circular confined jets," Journal of Fluid Engineering 125, 835-842 (2003)

xi. D.P. Mishra and S. K. Dash, "Prediction of entrance length and mass suction rate for cylindrical sucking funnel. International Journal of Numerical Methods in Fluids 63, 681-700 (2010).

xii. A.K Barik, S.K Dash and A. Guha, "New correlations for prediction of air entrainment into an Infrared suppression (IRS) device," Applied Ocean Research 47, 303-312 (2014).

xiii. H.A. Becker, H.C. Hottel and G.C. Williams, "Mixing and flow in ducted turbulent jets," In: 9th International Symposium on Combustion. Pittsburg (PA): The Combustion Institute, 7–20, (1963)

xiv. R. Pritchard, J.J. Guy and N.E.Conner, Industrial Gas Utilization, Bowker, New Providence, NJ. (1977)